

The Influence of the Radiation Effect of Louvred Screens on the Air Temperature Measurement

QIAN LIU^{1,2}, JIADE YAN^{1*}, JIANGXIA GUO³, FENG JIANG⁴, XIANKE YANG⁴, LIANJI JIN¹

¹ School of Atmospheric Physics, NUIST, Nanjing, China

² College of Applied Meteorology, NUIST, Nanjing, China

³ Meteorological Observation Centre, CMA, Beijing, China

⁴ College of Atmospheric Science, NUIST, Nanjing, China

Abstract

The radiation thermal effect of the radiation shield is one of the major factors which may cause deviations of the air temperature measurements. In the present study, by using the seasonal variation of the solar radiation in Nanjing, we used the computational fluid dynamics (CFD) software to investigate the radiation effect of the louvred screen, which is widely implemented in the meteorological observations in China. The impacts of the solar radiation and the correlations between the deviation of the temperature measurement and radiation absorption of the screen are discussed. The computational results show that the radiation deviation exhibits an “M”-shape diurnal variation due to the change of the solar radiation. Specifically, before 08:00, the deviation increases gradually, and then reaches a maximum value between 08:00 and 10:00. Afterwards, it decreases between 10:00 and 12:00. Aside from that, the deviation also shows a seasonal change. At 09:00 of the springtime and autumn, a maximum deviation, 0.7 °C, was found. In contrast to that, the minimum value occurs at 12:00 of summer, which has a value of approximately 0.2 °C. It was also found in simulations that due to the heating of the upper and lower shelves of the screen, the temperature inside the screen shows a “C”-shape distribution along the vertical direction. The temperature in the middle part is lower than that in the upper and lower parts of the screen. In addition, the temperature change in the middle part (0.15-0.35m) was found to be small, within the range of 0.1-0.2°C. The radiation deviation of the temperature was also found to be proportional to the solar radiation absorbed by the lateral sides of the louvred screen, and the correlation coefficient has a value of 0.93. The results obtained in the present study can be applied for the refinement of the structure of the louvred screen. Moreover, it also helps to improve the corrections of the existing temperature models.

Keywords: radiation effect; seasonal change; louvred Screens; air temperature measurement

Introduction

Temperature is the main essential factor in the conventional ground meteorological observation (XU Wei 2015 and TIAN Hong 2008), the observation method and the deviation are directly related to the understanding of atmospheric processes and forecast precision (YAN Jiade 2015; Zhao Bing 2010; CHEN Tao 2014). At present, the China meteorological administration

Supported by: National Natural Science Foundation of China (41505136) ; National Nonprofit Industry Research Foundation of China (GYHY201106049),

* Corresponding author: Jiade Yan, School of Atmospheric Physics, NUIST, 219 Ningliu Road, Pukou, Nanjing, China, 210044. Email: yanjd@nuist.edu.cn

has established throughout the country more than 55000 ground automatic weather stations (including national automatic station and regional automatic station), and the radiation protection device is popularly the fiberglass screen(YAN Jiade 2014). Screen is used to install protective equipment of temperature and humidity instrument, in order to prevent the instrument from the direct radiation and the reflection radiation of the ground, to protect the instrument from the effects of strong winds, rain, snow, etc, and make induction instrument parts with proper ventilation, can really sense the air temperature and humidity changes.

In temperature measurement, the radiation deviation always affects measurement accuracy. Radiation deviation refers to the deviation caused by the solar and ground direct radiation, in which the influence of solar radiation is most significant(WANG Ying 2002). When the screen after heated by solar radiation, affect the temperature field inside the screen, and there is no guarantee that the consistency of atmospheric temperature inside and outside of the screen, may lead to differences between observation and actual temperatures.

Many scholars at home and abroad have studied the temperature difference feature between inside and outside the screen, different screen observation data contrast, etc. Results show that: The heating errors increase with increasing shortwave radiation and diminish with increasing wind speed. The radiative heating is also found to be a function of sun elevation with maximum heating errors occurring at elevations of approximately 45° (Lin X 2001a and 2001b; Hubbard K G 2010; Anderson S P 1998). Ai-li Zhang etc, analyzed the screen structure on the influence of the temperature observations; Hai-hong Huang etc, mentioned in the analysis of the temperature characteristics inside and outside shelters and establishment of the prediction equation for the temperature outside the thermometer screen, because the large seasonal differences in the temperature of shelters, and therefore need to create a prediction equation of winter summer respectively; Steven p. Anderson is proposed, the radiation error curves exist bimodal structure, and has obvious difference in different seasons.

At present,there are few quantitative studies on temperature field and flow field distribution and seasonal differences in thermometer screen Quantitative study of seasonal differences in temperature of thermometer screen. Predecessors have researched the fluid dynamics analysis on solar radiation error of radiosonde temperature measurement, therefore we used the computational fluid dynamics (CFD) software to investigate the radiation effect of the louvered screen, which is widely implemented in the meteorological observations in China. The temperature changes inside the screen are mainly affected by direct solar radiation, and the stronger the radiation is, the more obvious the heating is. Therefore, by using the seasonal variation of the solar radiation in Nanjing(32°N , 118.8°E), under the condition of static stability, the basic characteristics of the radiation heat effect of the screen, the influence mechanism of flow field and temperature distribution in the screen, and the seasonal differences are analyzed. Moreover, the correlations between the deviation of the temperature measurement and radiation absorption of the screen are discussed. The results obtained in the present study can be applied for the refinement of the structure of the louvered screen. Moreover, it also helps to improve the corrections of the existing temperature models.

1 Materials and methods

The solar radiation error analysis of the screen includes 3D modeling, grid division, steady-state thermal analysis and general post-processing. In the process of analysis, the influence of solar altitude, azimuth angle, solar radiation intensity and screen material and other

parameters are considered(LIU Qingquan 2013; Mao Xiao-Li 2014).

1.1 Modeling and simulation

In this paper, the simulation of the main material of glass fiber reinforced plastic screen for unsaturated polyester resin and glass fiber cloth, four walls made of two rows of thin blades, the bottom is composed of three pieces of glass fiber reinforced plastic, each 110 mm wide, in the middle of a piece of a little higher than the edge two pieces, the box cover is composed of two layers of glass fiber reinforced plastic. In modeling, the rectangular coordinate system is adopted to define x,y and z direction respectively to the north, zenith direction, and the right east, and the temperature measuring element is set at the bottom of the thermometer screen at a height of 0.2 meters. At the same time, the thermometer screen structure is simplified without considering the screen door and the setting of the connecting rod and assuming the same four walls.

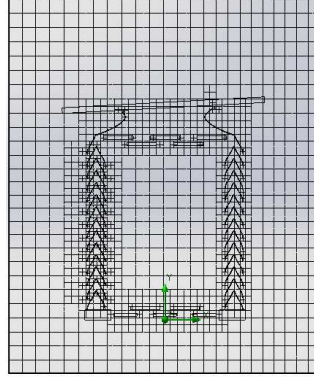


Fig.1 Schematic diagram of reinforced plastics screen mesh generation in the front view

In order to achieve high accuracy and computational efficiency, at the same time, the calculating equations can normal convergence, meshing set when the x, y, z direction of the grid number respectively, 24, 27, 24, tiny solid features refined level set to 3, x, y, z axis of the computational domain were 0.6 m-0.6 m, 1.2 m-0.2 m, 0.6 m-0.6 m. Forward-looking mesh of datum as shown in figure 1, the fluid grid number is 61394, 494 solid grid, can be seen from the figure in the glass fiber reinforced plastic screen and its surrounding air is relatively dense grid, and the regions with slower temperature changes were divided into more sparse meshes.

1.2 The steady heat conduction

1.2.1 Solar radiation intensity and direction

The solar altitude H_s and azimuth A_s are used to determine the position of the sun on the celestial sphere. H_s is the angle between the direction of the sunlight and the ground plane. The azimuth A_s defined here as positive south is 0, clockwise is positive, counterclockwise is negative. The calculation formula is respectively:

$$\sin(H_s) = \sin \varphi \cdot \sin \delta + \cos \varphi \cdot \cos \delta \cdot \cos \omega \quad (1)$$

$$\cos(A_s) = \frac{\sin(H_s) \cdot \sin \varphi - \sin \delta}{\cos(H_s) \cdot \cos \varphi} \quad (2)$$

Where φ is geographic latitude, δ is declination, ω is hour angle.

In the equatorial coordinate system, the sun position is determined by the declination and hour angle. Declination is the angle between the earth's equatorial plane and the connection to the center of the sun and the earth. Hour angle is from the observation point celestial meridian to the

sun's circle along the celestial equator. The calculation formula is respectively:

$$\delta = 23.45 \times \sin\left(360^\circ \times \frac{284+n}{365}\right) \quad (3)$$

$$\omega = 15 \times (ST - 12) \quad (4)$$

Where n is number of days, since January 1st of each year, ST is apparent solar time, in 24 hours. The time in this paper all refers to apparent solar time, i.e. local time.

Radiation errors are mainly generated by direct radiation from the sun and ground, while direct solar radiation is the main factor. At the same time, the effect of cloud and other sky conditions on the solar radiation is very important and cannot be ignored. When considering cutting calculation formula of solar direct radiation is:

$$I = I_0 \times P^m \quad (5)$$

Where I_0 is Solar radiation constant $1367\text{W}/\text{m}^2$, P is coefficient of atmospheric transparency, m is air mass.

$$m = \frac{1}{\sin(Hs)} \quad (6)$$

In order to facilitate the simulation parameters settings, this definition of azimuth As' as with the opening of the north direction of the target direction, the incident direction for termination direction of sunlight, the angle of the measured clockwise. According to the definition above, the solar radiation is in the x, y and z directions:

$$x = \cos(Hs) \cdot \cos(As') \quad (7)$$

$$y = -\sin(Hs) \quad (8)$$

$$z = \cos(Hs) \cdot \sin(As') \quad (9)$$

1.2.2 Screen radiation absorption

Based on the calculation formula of solar radiation absorbed by the radiation protection device, the formula of absorption radiation calculation based on the screen is proposed(Anderson S P 1998):

$$\alpha_s IA_0 = \alpha_s I [ld \sin Hs + h \cos Hs (l |\sin As'| + d |\cos As'|)] \quad (10)$$

Where α_s is the absorptivity of screen to solar radiation, take 0.3 here, I is the solar radiation intensity after considering cutting, A_0 is effective area of screen under the sun. Screen is 0.626 m long, 0.617 m wide, 0.890 m high.

1.2.3 Simulation parameter setting

In this paper, simulation experiment is mainly to analyze the seasonal change of solar radiation on the temperature distribution within the screen caused by the error, in order to eliminate the influence of other environmental factors, the simulation results without considering the environment temperature, wind speed, etc. The impact on the internal temperature of the

glass fiber reinforced plastic screen, so considering the wind speed is zero and select constant 26 °C ambient temperature. The specific physical parameters are shown in table 1.

Table 1 Physical parameter of reinforced plastics screen

Property	Value
density	1800kg/m ³
specific heat	1260J/(kg.K)
heat conductivity	0.4W/(m.K)
absorptivity	0.3
static pressure	101325.00Pa
relative humidity	50.00%
environment temperature	26°C

2 Results and analysis

2.1 The diurnal variation of radiation absorption

Changes of solar altitude, azimuth and hour angle on the summer solstice in Nanjing are shown in figure 2. It can be seen from the graph that the curve of the solar altitude diurnal variation is parabolic, and the solar altitude is 12.2° at 6 a.m & p.m, 81.4° at noon. Namely, it is the smallest at sunrise and sunset, largest at noon. Solar altitude in the morning and afternoon is symmetrical about 12 o'clock, affected by the geographic latitude, the sun does not radiate the top of louvered screen on the summer solstice in Nanjing. The curve of solar azimuth daily change is "S" type distribution, azimuth values are the same in the morning and afternoon but opposite in sign, and symmetrical about 12 o'clock, the solar azimuth is 0° at noon, the incident direction of the sun is in the screen south, azimuth is negative in the morning, the sun incident direction by east, azimuth is positive in the afternoon, the sun incident direction by west, and the sun azimuth is less than -90 ° from 6-8 a.m, the 16-18, and the solar azimuth is greater than 90 ° at 16-18 p.m, which accounts for that the north side of the screen is also exposed to the sun. The hour angle is linear changes, when the morning is negative, right in the afternoon, and 0° at noon, morning and afternoon is symmetrical about 12 o'clock, hour angle is -90 ° and 90 ° at 6 a.m and 18 p.m respectively.

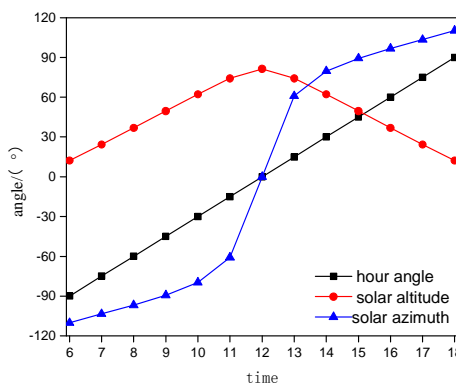


Fig 2 Changes of hour angle, solar altitude and azimuth on the summer solstice in Nanjing

The solar direct radiation and screen absorption of solar radiation are shown in figure 3, figure 3 (a) illustrates the solar direct radiation intensity curve, (b) the effective area curve of screen under the sun, (c) screen total solar radiation, the top absorb solar radiation absorption and side absorption of solar radiation change curve. By figure 3 (a) can see, the sun direct radiation intensity curves are parabolic, sunrise and sunset, the sun direct radiation intensity is smaller, at noon the sun direct radiation is strongest, 12 o'clock is strongest when the solar direct radiation

is 903.5 W/m^2 , 06 and 18 when the solar direct radiation is only 196.1 W/m^2 , symmetrical about 12 in morning and afternoon. From figure 2, the solar altitude is smaller at sun sunrise and sunset, the sun radiation through the atmosphere to a longer path on the surface of the earth, the sun directly radial cutting is stronger by atmospheric cloud cover, solar altitude at noon is the largest, best solar direct radiation. From figure 3 (b), curve of effective area the screen can absorb the solar radiation is "V" -shape, effective area is 0.46 m^2 minimum at 12 o'clock, 06 and 18 when the effective area of 0.78 m^2 maximum, and symmetrical about 12 in morning and afternoon. From figure 3 (c), screen absorption of solar radiation is also about 12 symmetrical, the overall absorption of solar radiation and the profile curve of absorption of solar radiation are "M"-shape, namely a bimodal type change, but the peak times are different, when the corresponding total absorption peak at 10 and 14, the absorption of solar radiation is 166 W , side absorption peak at 8 and 16, absorb solar radiation of 102.5 W , the trough of the solar radiation absorption at 12, total absorption radiation wave trough of 125.7 W , side absorb radiation wave trough of 22.1 W . And roof to absorb solar radiation changes for the parabolic, along with the solar altitude in the morning and the sun direct radiation intensity increasing, the top absorption of solar radiation also increases gradually, 06 at least 4.8 W , 12 when the solar altitude and the sun direct radiation intensity largest, roof absorption of solar radiation achieve maximum 103.5 W as well, with the solar altitude gradually reduce in the afternoon, the top is less absorption of solar radiation as well. Screen to absorb the total solar radiation is of top solar radiation and side absorb solar radiation combined.

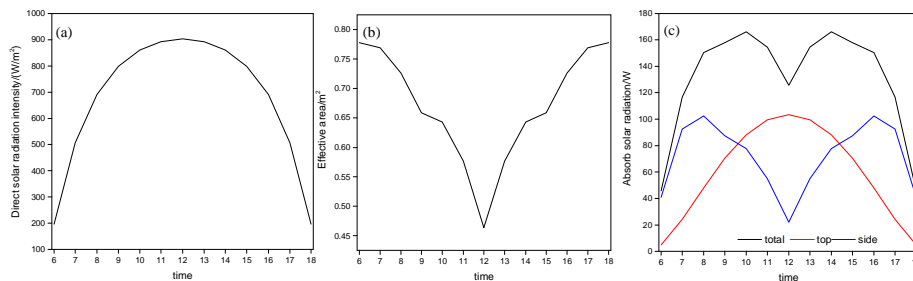


Fig 3 Changes of direct radiation intensity (a), screen effective area (b), solar radiation absorption (c) on the summer solstice in Nanjing

From the above analysis, shows that the strength and direction of the sun as well as the screen absorb solar radiation are symmetrical about 12 o'clock, the value of morning and afternoon solar altitude, azimuth, the intensity of solar radiation and the screen to absorb solar radiation is the same, but the symbols of solar azimuth is on the contrary, by east in the morning, azimuth negative, by west in the afternoon, the azimuth is positive. Overall absorption of solar radiation and the profile curve of absorption of solar radiation are in "M" type, and head to absorb solar radiation changes for the parabolic.

2.2 Thermal effect of screen wall

Numerical simulation for temperature velocity field distribution is shown in figure 4. A, B, C, respectively represent front datum, right on the datum and datum, (A) to (g) respectively 6-12.

From figure 4 temperature field can be intuitively seen, sun radiate effect of screen has the features of the diurnal change, the temperature of the walls of the morning showed a trend of decrease after the first increase, 12 at the minimum, the maximum amplitude of warming side blade can reach more than $4 \text{ }^\circ\text{C}$; Increasing the temperature of the roof, 12 when maximum, minimum when 06, screen near the walls and roof air temperature is much higher than inside the screen; Can be seen from the air flow direction, the radiation effect of non uniformity make the

internal, the phenomenon of the annular flow field.

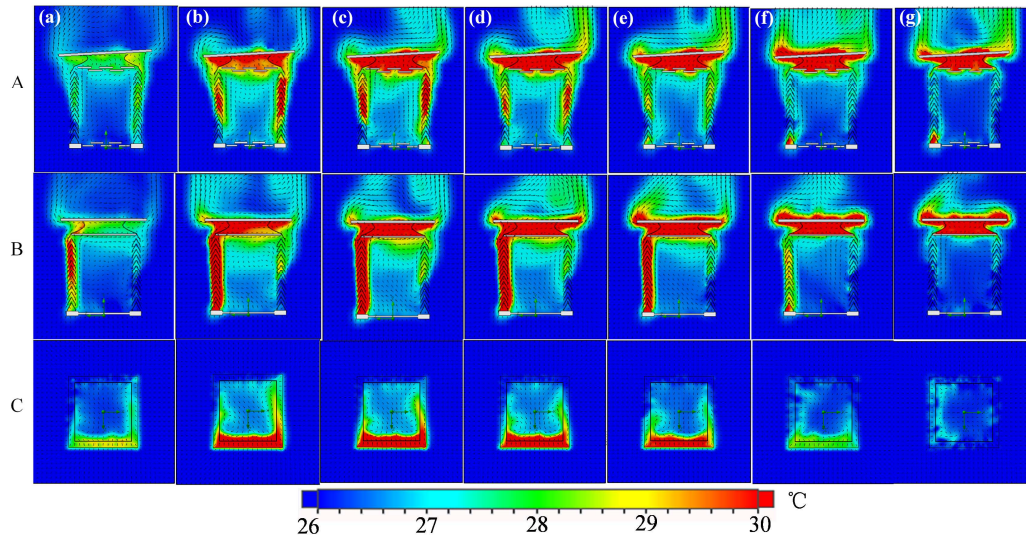


Fig 4 The temperature field and flow field distribution of the screen on the summer solstice in Nanjing
A front plane, B right plane, C top plane, (a)~(g) 06:00~12:00

2.3 Vertical distribution of temperature difference

In order to study the distribution of the internal temperature of the screen, select the five directions: temperature measuring element location, distance measuring temperature element 0.1 m in the east, south, west and north four bearing vertical height, defined as temperature difference $\Delta T = T_s - T_a$, T_s for measuring temperature, T_a as air temperature, and change of ΔT at the different time with the height as shown in figure 5, (a) to (g) respectively represent 6-12.

In figure 5 (a)-(g) can be intuitive to see, ΔT inside the screen shows a "C"-shape distribution along the vertical direction. The temperature in the middle part is lower than that in the upper and lower parts of the screen. Under 0.15 m part has a "bump", namely the temperature significantly higher than the ambient temperature. This is because the affected by screen base, due to the heating of the lower shelves of the screen, five directions vertical height under 0.15 m part are at higher temperature in different time. Including 6, 8, 10, 11 and 12 is when the temperature is highest in the south.

In 0.15 m height above the space, can be seen from the change over time as the ΔT , ΔT showed a trend of decrease after the first increase, the maximum 08 at 1.0 °C, 12 when the minimum is 0.3 °C. This with figure 2 (c) the changing trends of the side absorb solar radiation, 08 side absorb solar radiation when peak, because of the heat conduction effect, ΔT is also the biggest, 12 when side absorb the least radiation, the ΔT is the smallest. As the middle section (0.15 ~ 0.35 m) ΔT changes with height is relatively slow, in addition to the 6 and 11, other times when not much change on the whole, all within 0.5 °C. In 0.35 m height above is affected by the upper shelves of the screen, ΔT increased with the increase of height sharply, range were greater than 0.5 °C. Known from the analysis of wall thermal effect, the air is heated up to the top of the air circulation, thus closer to the top, the higher the temperature, the greater the temperature difference to the environment.

Five directions at the same time when there exist obvious differences in temperature difference of vertical height, in addition to the 10 and 11, is a temperature measuring element location vertical height (axis) as the ΔT is minimal. At between 0.1 m and 0.25 m height minimum as the north ΔT is 0.4 °C, at between 0.25 m and 0.4 m height minimum as the east side of ΔT is 0.3 °C, but the north and the east and the central axis of the difference is less than

0.1 °C. At 06, 07, and 10, it is the largest of the south side, while 08 and 09 north ΔT is the

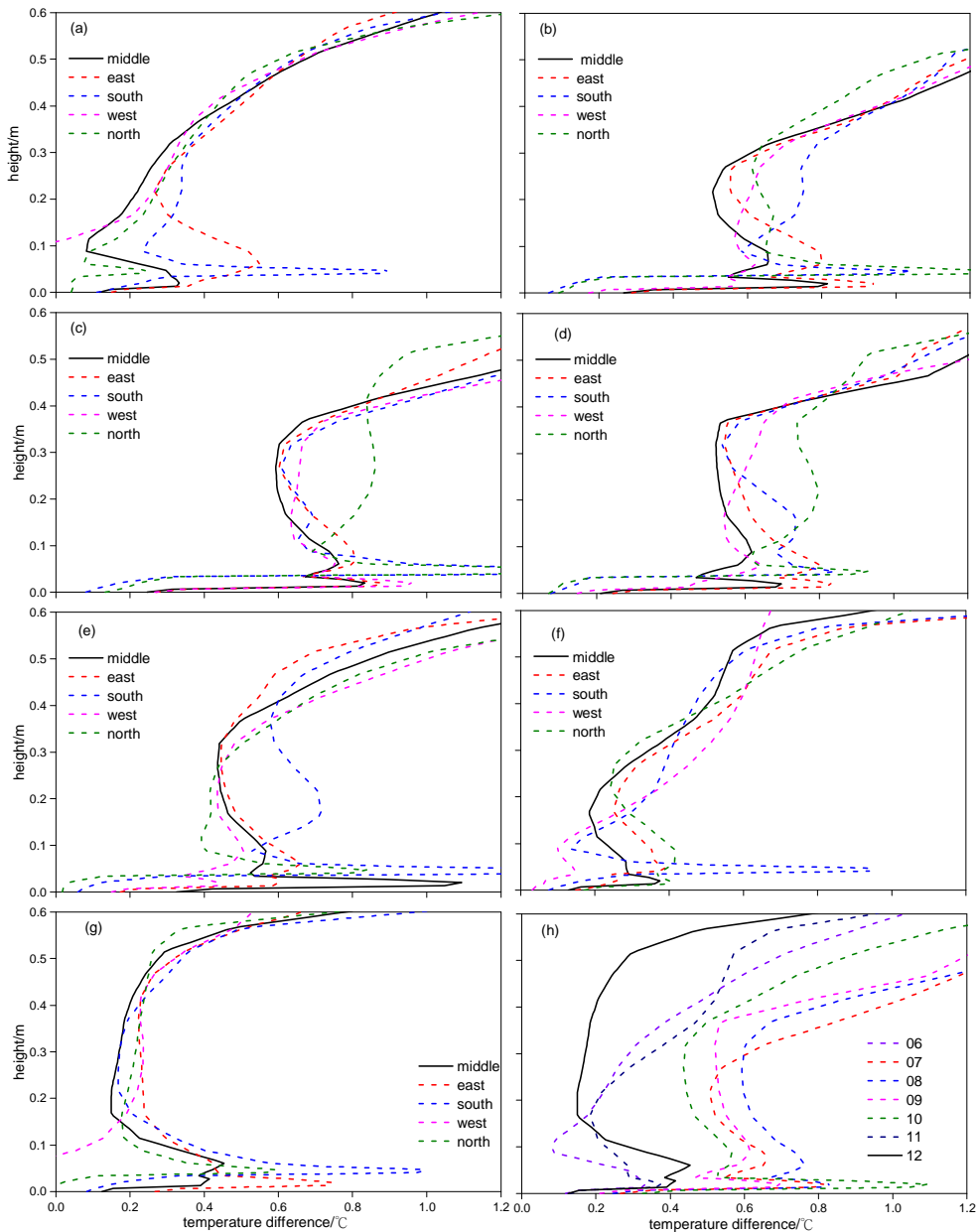


Fig 5 Temperature differences profile over time and direction within the screen on the summer solstice in Nanjing
(a)-(g) 06:00-12:00, (h) on the central axis

largest, at 11 the west side of ΔT is 0.6 °C, the maximum at 12, when the ΔT is between 0.2 °C to 0.3 °C five directions. In part of 0.35 m above, the temperature difference between the five directions is, within 0.1 °C. Because of the closer to the top, the higher the temperature, different position as the ΔT is larger, the difference is not obvious. When the 07, 08, 09 and 12, the north ΔT is smaller.

The above analysis shows that, generally speaking, the minimum ΔT on the central axis, so the vertical distribution of temperature on the central axis at different time is shown in fig.4 (h). It shows that upper the part of 0.15 m, 12 when the ΔT is always the smallest, is less than 0.5 °C, 07 and 08 is one of the biggest, the range between 0.5 °C-2 °C.

In order to study the seasonal differences inside the screen, the temperature distribution in the central axis of the screen is selected as the object of study. The vertical distribution of the radiation error in the central axis is measured in each season between 6:00 and 12:00, and the daily variation curve is shown in figure 6.

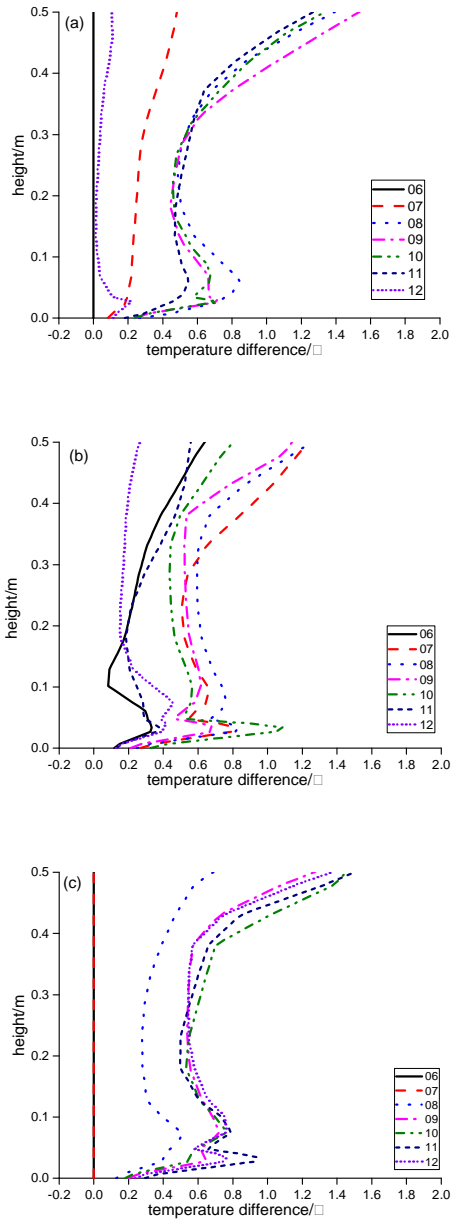


Fig. 6 Vertical diurnal variation of temperature error in each season:

(a) spring (autumn);(b) summer;(c) winter

There is obvious difference among the seasonal variation curves of deviation in the central axis of the screen. Generally, the diurnal variation is most obvious in the larger in 0.35 ~ 0.5m.

summer, which reaches 0.6°C in the middle part, while the corresponding temperature change is relatively small in the spring (autumn) and winter, which is less than 0.3 °C . The deviation is biggest in the summer before 8:00 in each season, which starts to reduce after 8:00. Meanwhile, the deviation in the spring (autumn) and winter continues to increase. By 12:00, the deviation in summer is the smallest, and the deviation in the winter is the biggest.

The solar radiation intensity in the spring (autumn), summer and winter was 494.08W / m², 690.75 W / m² and 196.85 W / m², respectively, and the temperature difference in the central axis of the louver was analyzed. In summer, the solar radiation is the largest, and the temperature error in the spring (autumn) season is the second. The temperature error in winter is the smallest. Therefore, the temperature error in the central axis of the summer is the largest, and the spring and autumn are which is the smallest in winter.

Between 9:00 and 10:00, the deviation in the central axis of the summer is gradually reduced while it continues to increase in spring (autumn) and winter. This is mainly because the sun elevation angle in spring (autumn) and winter is smaller, and meanwhile, the sun irradiates directly to the side of the screen. However, the sun elevation angle is high in the summer. As the elevation angle continues to increase, the direct position of the solar radiation has gradually moved from the side wall to the top. And the top radiation and heat insulation effect is much better than the side wall. Therefore the summer radiation error gradually reduced. From the vertical change point of view, the difference of deviation in the 0.15 ~ 0.35m is smaller while it's

Between 11:00 to 12:00, the deviation in the summer continues to decrease and its deviation is the smallest compared to other seasons while it's largest in the winter. In the case of noon at 12:00, the sun elevation angle in spring (autumn), summer and winter are 57.60 °, 81.45 ° and 34.56 °, respectively. The sun elevation angle in the spring (autumn) and winter ranges is small, so the solar radiation irradiates directly the side wall mainly. In the summer, the sun has a high elevation angle and the solar radiation is directly on top of the screen. The top of the screen is much better than the side wall in terms of insulation effect, which leads to the result that the deviation in summer is the smallest. At 12:00, the seasonal variation of the deviation in the central axis is the most obvious.

2.4 Daily variation of temperature difference

In order to compare the change of temperature at different positions in the summer solstice, the temperature difference of the five points in the center, east, south, west and north of the 0.2 m height of screen is studied. When summer solstice 6-18, height of 0.2 m, five points of the diurnal variation of the temperature difference is shown in figure 7.

It is observed that for the five locations, the daily variation of temperature difference of bimodal type, curve is "M" type change, and the profile curve of absorption of solar radiation in figure 3 change trend. In the lower solar altitude, the path of the sun radiation through the atmosphere to the ground is longer, the sun's radiation cut more, so at 6 and 18 when the sun radiation caused by the radiation deviation is small, between 0.2 °C to 0.3 °C. 6-8 when the intensity of solar radiation is the dominant factor, increased from 196.1 W/m² to 690.7 W/m², so the side absorption of solar radiation is increasing. The five point temperature difference inside the screen also increases. 09-12 when screen absorb solar radiation effective area is the dominant factor, solar altitude is rising, increased from 49.6 ° and 81.4 °, although the intensity of solar radiation is also increasing, increased from 798.2 W/m² to 903.5 W/m², but 9-12 when the solar altitude is always greater than 45 °, 12 when the sun light mainly hitting the screen roof, the walls of the effective area decreases, absorption of solar radiation has been reduced, so the screen within five points of difference in temperature and decreases, is minimum, when 12 between 0.2 °C to 0.3 °C. Likewise, in the afternoon, 12-16 when the solar altitude gradually decreases, the radiation deviation caused by solar radiation gradually increase, at 16 when maximum 0.6 °C to 0.8 °C. 16-18, when the intensity of solar radiation is the dominant factor, the solar altitude is less than 45 °, the intensity of solar radiation by 690.7 W/m² reduce to 196.1 W/m², as a result, the radiation deviation caused by solar radiation also gradually become smaller, 18 to minimize, between 0.2 °C to 0.3 °C.

By comparing the same time when the difference in temperature between five position can be seen that, overall, intermediate point the minimum temperature difference among them, 12 of the minimum, less than 0.2 °C. The north point of the temperature difference is bigger, reached the maximum at 8 and 16, more than 0.8 °C, this is because at 6-8 when the sun azimuth is always less than 90 °, sunrise on the summer solstice, the sun's rays is far north, from the top view of the temperature distribution can be seen, 6-11, on the east side of the temperature is always greater than the north, the heated air flow faster, wall heat decreases, and the temperature is less than the east, on the northern side of the air flow speed slower, quantity of heat in the north, north of caused by temperature difference is bigger. Can be seen from the temperature distribution on the top view, due to the wall thermal effect, the closer the enclosure, the higher the temperature, at the same time, according to the results of the analysis in the vertical distribution of the temperature difference, in the part of 0.15-0.35m at different time, temperature difference on the central axis is the smallest, so in general, as in the middle of the ΔT compared with the other four

points is the smallest, and at 12 when is the smallest.

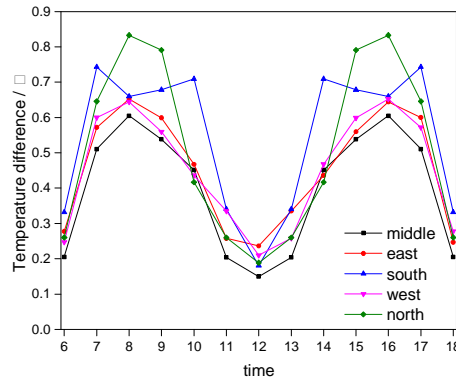


Fig 7 Diurnal variation of temperature differences within the screen on the summer solstice in Nanjing
The diurnal variation curve of the radiation error at the point of the temperature measurement element is analyzed. The results are shown in Fig.8.

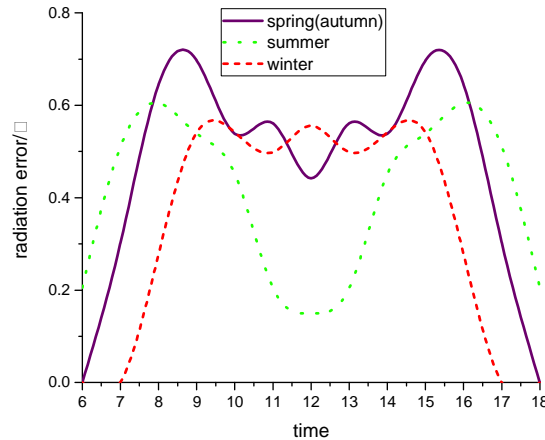


Fig.8 Daily variation analysis of radiation error

In Fig. 8, the diurnal variation curve of radiation error in each season has the "M" type bimodal structure with 12:00 symmetry. The diurnal variation curves of radiation error reach the peak between 8:00 and 10:00, while the valley appears at noon except the winter. Compared with the diurnal variation curve of radiation error in each season, it was found that the bimodal structure was the most obvious in summer, and the difference between peak and valley could reach 0.45 °C while the bimodal structure in spring and autumn are not obvious, which is less than 0.25 °C. This is in line with the results of Steven P. Anderson. Steven P. Anderson compared the solar radiation heating and the deviation caused by radiation at 15.5 °N on 15 May and 15 November, and found that the bimodal structure was more pronounced in May than that in November since the sun elevation angle was low in November.

2.5 Correlation between radiation absorption and temperature difference

Due to the screen wall thermal effect, the absorption of solar radiation by the screen is the main factor that causes the internal temperature measurement deviation. Diurnal change of screen side and overall solar radiation absorption show a "M"-shape distribution, the top absorb solar radiation shows parabola change, correlation between radiation absorption and middle, east, south, west and north five position ΔT are shown in table 2. Can be seen from table 2, correlation

between the side absorption and the ΔT inside the screen reached extremely significant level, while the roof of screen and total radiation absorption and ΔT , there is no significant correlation, that is more than 99% of the probability of that there is a correlation between the radiation absorption of the side screen and ΔT

Table 2 Correlation between radiation absorption of screen and temperature difference

correlation coefficient	lateral sides	upper screen	overall
middle	0.966 ^{**}	-0.158	0.472
east	0.963 ^{**}	-0.175	0.454
west	0.970 ^{**}	-0.188	0.448
south	0.926 ^{**}	-0.151	0.453
north	0.913 ^{**}	-0.209	0.393

(note: ^{**} reached a significant level)

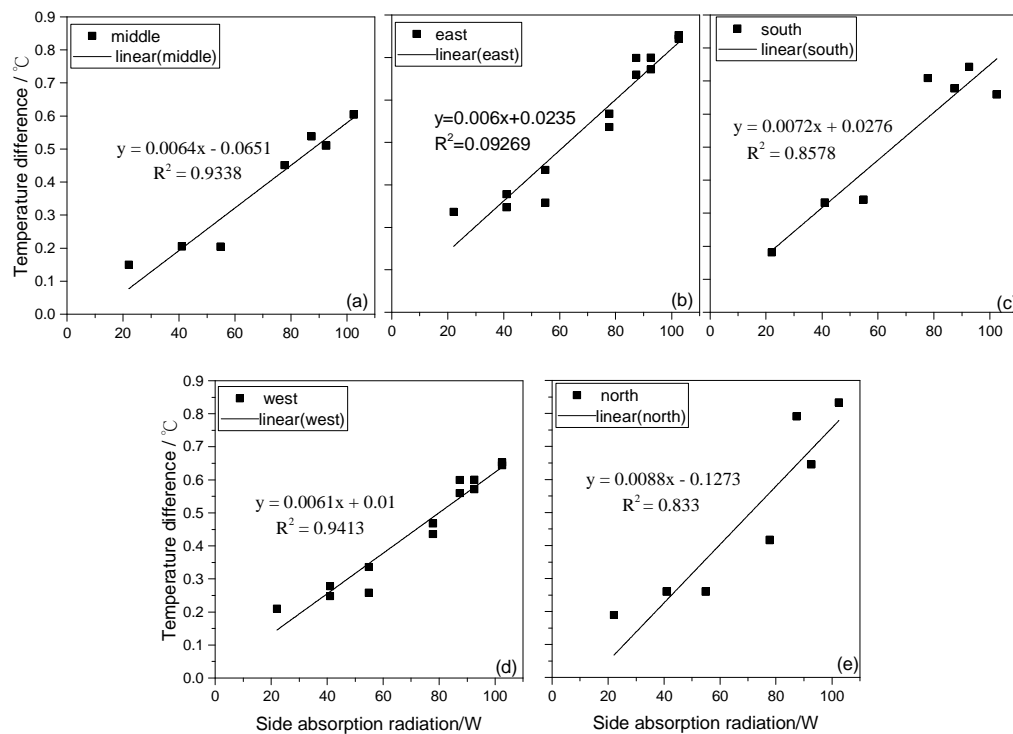


Fig 9 Scatter diagram of screen lateral absorption radiation and radiation deviation

Casing side blade radiation absorption and air temperature observation deviation of scatter plot as shown in figure 9, seen from the figure, ΔT of the different points and side radiation absorption are linearly dependent, but fitting results with a certain deviation between the actual value, when no side absorb radiation, still there is temperature difference to the environment. Therefore, mathematical statistics method are used to get the side screen radiation absorption and the position of five linear fitting equation and the confidence interval can be seen in table 3, the regression equation of y as said ΔT (unit: °C), x for screen side absorb radiation (unit: W), confidence interval refers to the scope of regression coefficient, represents the deviation between the fitting result and the measured value. From the table, in the middle of the temperature difference is not the best fitting effect, on the west side of the temperature difference between side absorb radiation and the best fitting effect, decision coefficient is 0.941, the correlation coefficient is 0.970.

Table 3 Fitting equation of lateral absorption radiation and radiation deviation in different azimuths

direction	fitted equation	determination coefficient R^2	95% confidence interval	
			lower limit	upper limit
middle	$y = 0.006x - 0.065$	0.934	-0.152	0.022
east	$y = 0.006x + 0.023$	0.927	-0.061	0.108
west	$y = 0.006x + 0.010$	0.941	-0.067	0.087
south	$y = 0.007x + 0.028$	0.858	-0.121	0.176
north	$y = 0.009x - 0.127$	0.833	-0.327	0.073

3 Summary and discussion

Application of computational fluid dynamics CFD simulation technology of glass fiber reinforced plastic screen effect of solar heat hot numerical simulation analysis, analyzes the basic features of the radiation effect of the screen, and the influence mechanism of the flow field and temperature distribution in the screen, and the correlations between the deviation of the temperature measurement and radiation absorption of the screen are discussed. Main results are as follows:

(1) The thermal effect of solar radiation is one of the main factors that cause the temperature observation error of thermometer screen, and has obvious daily and seasonal variation characteristics. The screen showed a trend of first increases and then decreases, the maximum amplitude of warming side blade can reach more than 4 °C; The temperature of the top is increasing in the morning and decreasing in the afternoon. The temperature of the air near the screen and the top cover is much higher than that in the thermometer screen. The non-homogeneity of radiant heat effect causes annular flow field inside the screen, which is most obvious at the time of 08 and 16, and the airflow rate is about 0.06 m/s.

(2) Each season to screen shows a “C”-shape distribution along the vertical direction. The temperature in the middle part is lower than that in the upper and lower parts of the screen. But there are obvious differences in daily trends, the daily change of the central axis in the summer is most obvious, the most obvious diurnal variation in 0.1-0.3 m height can reach 0.6 °C, the diurnal variation of the spring season (fall), winter is relatively small, both within 0.3 °C.

(3) The radiation deviation exhibits an “M”-shape diurnal variation due to the change of the solar radiation. Specifically, before 08:00, the deviation increases gradually, and then reaches a maximum value between 08:00 and 10:00. Afterwards, it decreases between 10:00 and 12:00. Aside from that, the deviation also shows a seasonal change. At 09:00 of the springtime and autumn, a maximum deviation, 0.7 °C, was found. In contrast to that, the minimum value occurs at 12:00 of summer, which has a value of approximately 0.2 °C.

(4) The radiation deviation of the temperature was also found to be proportional to the solar radiation absorbed by the lateral sides of the louvered screen, and the correlation coefficient has a value of 0.93.

This paper analyzes the fiberglass screen cause error of radiation temperature measurement, only consider the influence of solar direct radiation, ignoring the different underlying surface reflection scattering solar radiation, the sun radiation and the ground long-wave radiation influence on error, which remains to be further improved.

References

- (1) XU Wei, HU Zhenqin, XIA Li, ZHU Chao, HU Ping, et al. Comparative Study on Temperature of Light Louvred Screen and Reinforced Plastics Screen. *Meteorological Monthly*, 2015, 41(2):240-246.

- (2) TIAN Hong, JIANG Shuangwu, LU Jun. The homogeneity test on mean annual precipitation and temperature over the Changjiang River and the Huaihe river basins. *Scientia Meteorologica Sinica*(in Chinese), 2008, 28(2):227-231.
- (3) YAN Jiade, WANG Chenggang, JIN Lianji, WANG Weiwei, et al. A Comparative and Modification Study of Louvred and Aspirated Shield Temperature Systems. *Climatic and Environmental Research*. 2015, 20(5):533-543.
- (4) Zhao Bing, Zheng Qinghua, Ye Xingrong, Lin Wei ,Lu Huabiao .The differences between the observations at the new and the old reference climatological stations in Nanjing, *Scientia Meteorologica Sinica*(in Chinese), 2010, 30(4): 559-563
- (5) CHEN Tao, YE Chengzhi, LI Chao, et al. Comparison of the temperatures between automatic instrument recording and manual observation in Hengyang city. *Scientia Meteorologica Sinica*(in Chinese), 2014,34(1):112-118.doi:10.3969/2012jms. 0155
- (6) YAN Jiade, JIN Lianji, WANG Weiwei, et al. Comparisons of the different temperature observing systems of second generation AWS. *Scientia Meteorologica Sinica*(in Chinese). 2014, 34(1):60-65
- (7) China Meteorological Administration. Surface meteorological observation standard. Beijing: Meteorological Press, 2003: 35-47.
- (8) WANG Ying. LIU Xiaoning. Comparative analysis of AWS and man-observed temperatures. *Journal Of Applied Meteorological Science*. 2002, 13(6): 741-748.
- (9) Lin X, Hubbard K G, Walter-Shea E A. Radiation loading model for evaluating air temperature errors with a non-aspirated radiation shield[J]. *Transactions of the Asae American Society of Agricultural Engineers*, 2001a, 44(5):1299-1306.
- (10) Hubbard K G, Lin X, Walter-Shea E A. The effectiveness of the ASOS, MMTS, Gill, and CRS air temperature radiation shields[J]. *Journal of Atmospheric & Oceanic Technology*, 2010, 18(6):851-864.
- (11) Anderson S P, Baumgartner M F. Radiative Heating Errors in Naturally Ventilated Air Temperature Measurements Made from Buoys*[J]. *Journal of Atmospheric & Oceanic Technology*, 1998, 15(1):157-173.
- (12) Thomas C K, Smoot A R. An Effective, Economic, Aspirated Radiation Shield for Air Temperature Observations and Its Spatial Gradients[J]. *Journal of Atmospheric & Oceanic Technology*, 2013, 30(3):526-537.
- (13) Mauder M, Desjardins R L, Gao Z, et al. Errors of Naturally Ventilated Air Temperature Measurements in a Spatial Observation Network[J]. *Journal of Atmospheric & Oceanic Technology*, 2008, 25(11):2145-2151.
- (14) Lin X, Hubbard K G, Waltershea E A, et al. Some Perspectives on Recent In Situ Air Temperature Observations: Modeling the Microclimate inside the Radiation Shields[J]. *Journal of Atmospheric & Oceanic Technology*, 2001b, 18(9):1470-1484.
- (15) Zhang Aili, Su Feng, Sun Zihui. Influence of Large and Small Louvered Screens on Temperature Measurements. *Meteorological Science and Technology*. 2013, 41(2):270-273.
- (16) HUANG Haihong, LING Ying, DONG Huiqing. Analysis of Inside and Outside Thermometer Shelter Air Temperature Characteristics in Nanning. *Meteorological Monthly*, 2003, 29(12):25-28.
- (17) LIU Qingquan, DAI Wei, YANG Rongkang. ZHANG Jiahong, LI Min. Fluid Dynamics Analysis on Solar Radiation Error of Radiosonde Temperature Measurement. *Plateau Meteorology*, 2013, (04):1157-1164.
- (18) Mao Xiao-Li, Xiao Shao-Rong, Liu Qing-Quan, Li Min, Zhang Jia-Hong. Fluid dynamic analysis on solar heating error of radiosonde humidity measurement. *Acta Physica Sinica*. 2014, (14):202-214.
- (19) China Meteorological Administration. People's Republic of China meteorological industry standard. 2013-07-11.